Journal of Membrane Science & Research

journal homepage: www.msrjournal.com

Research Paper

Thin Film Nanocomposite (TFN) Membrane Comprising Pebax®1657 and Porous Organic Polymers (POP) for Favored CO_2 Separation

Fatemeh Ranjbar, Mohsen Ghorbani, Reza Abedini *, Mitra Ghasemi

Faculty of Chemical Engineering, Babol Noshirvani University of Technology, Shariati Ave, Babol, 47148 71167, Iran

Article info

Received 2021-08-09
Revised 2021-10-26
Accepted 2021-10-30
Available online 2021-10-30

Keywords

Thin film nanocomposite (TFN)
Pebax®1657
Porous organic polymer (POP)
CO_2 separation

Highlights

- Novel TFN membranes (MMMs) for CO_2/CH_4 separation.
- Porous organic polymers incorporated with Pebax to improve CO_2 permeability.
- The Pebax/POP TFN membranes showed superior separation performance.

Graphical abstract

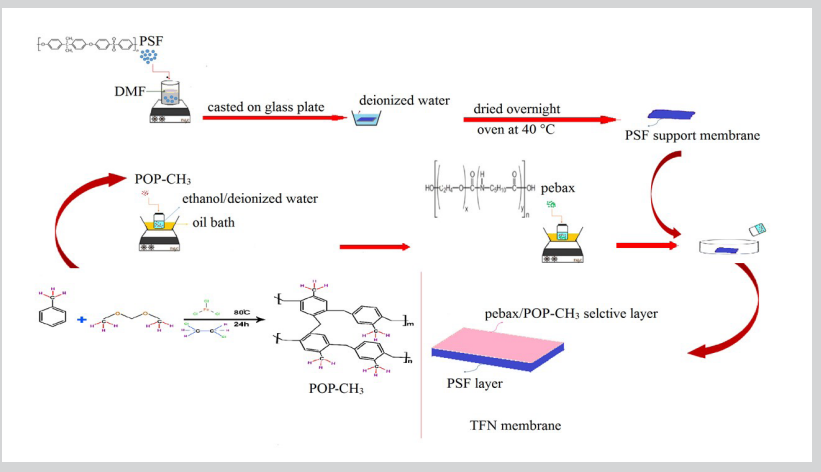

Abstract

Global warming is a public alarming issue caused by extreme CO_2 emissions. Thus, CO_2 removing using thin film nanocomposite (TFN) membranes is an efficient procedure to enhance the CO_2 gas separation efficiency. TFN membranes composed of Pebax 1657 embedded by porous organic polymers over the porous polysulfone support used to separate CO_2 from CH_4 and N_2 gases. Porous organic polymers (POPs) were synthesized via Friedel-Crafts one-step reaction. The obtained results from TGA and FESEM revealed that the modified TFN membranes declared a superior compatibility between Pebax and fillers. Permeation properties of membrane samples were tested over various feed pressure with the range of 2-10 bar. Pure gases permeability, CO_2/N_2 and CO_2/CH_4 selectivities improved via adding porous organic polymers into the Pebax. At porous organic polymers loading of 5wt% and applied feed pressure of 2 bar, the CO_2, CH_4 and N_2 permeability enhanced to 310.6, 27.6 and 4.5 Barrer, respectively; which exhibited a significant improvement compared to neat membrane. Moreover, the CO_2/N_2 and CO_2/CH_4 selectivities also enhanced to 11.25 and 70.04; respectively. Obtained results revealed that the membranes performance was enhanced as the feed gas pressure increased. TFN containing 5wt% porous organic polymers imply a CO_2 gas permeability of 348.4 Barrer at feed pressure of 10 bar.

1. Introduction

Nowadays, global warming, due to the increase of greenhouse gases emission and its excessive destructive effects, has become an essential issue. Unfortunately, there are numerous greenhouse gases such as nitrous oxide, water vapor, methane, carbon dioxide and etc. which have led to the public health issues and environmental pollution. The increasing rate of using fossil fuels to provide the required energy demand, causes the extreme CO_2 emission. Thus, seeking a solution to prevent the CO_2 emission is a vital concern that eventuate to environmental refinement [1-4]. Moreover, the carbon dioxide separation from methane is one of the most essential tasks in gas refining plants. The attendance of carbon dioxide in natural gas leads to the corrosion problems and also decreases the heating value of refined gas [5].

Carbon dioxide removing methods involving absorption, adsorption and refrigeration which rely on operating condition, economics, and processes manner [6-9]. Among these methods, membrane technology in gas separation industries considered and developed as a result of the its simplicity operation, less energy demand and low conservation cost and was regarded as the most admiring method to remove carbon dioxide from gas streams during the past few decades [10-13]. However, depends on the CO_2 destination after

* Corresponding author: abedini@nit.ac.ir (R. Abedini)

DOI: 10.22079/JMSR.2021.535579.1485

separation, sometimes a large compression train would be required, entailing much higher power consumption than other technologies that produce high pressure CO_2.

Membrane performance depends on their inherent materials properties. Among various materials for membrane fabrication, polymers are reasonable candidates for CO_2 capturing and natural gas sweetening due to their sufficient advantages including lower fabrication cost, several modules design (i.e., hollow fiber, plate and frame, spiral wound), great variety of materials and feasible changes in their physicochemical properties [14]. In membrane gas separation processes, both selectivity and permeability are the most important parameters and their tradeoff was presented by Robeson upper bound [10,15]. Polymeric membranes travail from this trade-off that sometimes restricted their usage in industrial application [16,17]. Thus, besides the polymers type utilized for membrane synthesis, several studies have been focused on the membrane structure design. Among suggested structures, TFN membranes consist of a thin dense layer filled by nanoparticles which supported by porous bottom layer have gained more concern. The low resistance against gas transport in porous support and thin selective layer could enhances the gases permeability in TFN membranes [18]. In TFNs, the thin selective layer has a significant role in overall selectivity gained by membranes. To improve the selective layer of TFNs, there are several available fillers categories such as carbon derived materials, metal organic frameworks (MOFs) [19,20], zeolite [21,22], hypercross-linked polymers (HCPs) [23-25], and covalent organic frameworks (COF) [26] that can be used to embed within the polymer matrix that ultimately enhances the performance of membrane. Dorosti et al. investigated the impact of Fe-BTC as a filler on the Pebax®1657 gas separation performance. Gas permeabilities increased by inclusion of Fe-BTC due to high CO_2 affinity of filler. Nafisi and Hägg [27] investigated the pure CO_2, CH_4, N_2, permeability via adding ZIF-8 particles into the Pebax matrix. The gas permeabilities increased and the CO_2/N_2 selectivity reached to 32.3 for Pebax membrane containing 35 wt. % ZIF-8. Mozafari et al. [28] examined the TFN comprising Pebax/Zr-MOFs over PMP sublayer for CO_2/CH_4 selectivity. The CO_2/CH_4 selectivity and also CO_2 permeability were 39.8 and 393.8 Barrer respectively, for modified TFN membranes embedding 1.5 wt.% of UiO-66-NH_2 at applied pressure of 700 KPa.

The quality of polymer/filler interface in TFNs and mixed matrix membranes could influence significantly on the efficiency of gas separation. A poor quality of filler/polymer interface leads to the formation of microvoids which act as non-selective medium for gas transport through the membrane. Neuromas studies have been performed to solve this problem which ultimately terminates to the several approaches such as using coupling agent [29,30], crosslinking of polymers [17], using compatible fillers with polymers [31], fillers functionalization [32] and etc. Among them, incorporating fillers those compatible with polymers is more easy and convenient approach. These fillers such as metal organic frame work (MOF), covalent organic frame work (COF) and porous organic polymers (POP) owing to their organic nature can interact with polymer chains and reduce the possibility of microvoids formation as can be possible.

A significant category of such materials is porous organic polymer (POP) with intrinsic characteristics such as high surface area and unique structure. The formation of covalent bonds in POPs can result in thermo-chemical stability and prevent the destruction and collapse the framework [33].

The effect of POP (2Ph) obtained from biphenyl monomer on gas separation performance of polycarbonate (PC) was investigated by Jardon et al. [34]. The POP added into the PC matrix by 10, 20 and 30 wt.% and the CO_2, CH_4 and N_2 permeability was measured for all MMMs. The permeability of all studied gases increased as the POP increased from 10 to 30 wt.%. The PC/2Ph (20 wt.%) MMM showed the best CO_2/N_2 and CO_2/CH_4 selectivity of 26.3 and 21.0, respectively.

Soto et al. studied the gas separation performance of MMM comprising copolyimide (copolymerized from APAF and 4,40-(hexafluoroisopropylidene) diamine (6FpDA)) and POP. The permeability of all tested gases (i.e., CH_4, CO_2, N_2, H_2 and O_2) increased as the membrane embedded by POP particles. The CO2/N2 and CO_2/CH_4 selectivities showed minor decreases. For H_2/CH_4 and H_2/N_2 separations with membranes approaching the 2008 Robeson's trade-off line [35].

POPs, with porous structure and surface-adjusted cavities are privileged candidates to incorporate with the selective layer and consequently improve the TFN membranes performance for efficient CO_2 separation [36-39]. Another essential issue is that, similar to the traditional one-layer membrane, the TFNs performance also is a great function of materials used in membrane fabrication. Among studied polymers, polysulfone (PSF) is often preferred as it showed premiere gas permeability and selectivity, proper thermomechanical resistance, low density, and good plasticization stability. Therefore, all these distinctive properties make PSF as an appropriate polymer for membrane development [40,41]. Moreover, polyether-block-amide (Pebax) is one of the promising polymers for CO_2 gas separation. Pebax composes of polyether (PE) and polyamide (PA) fragments. PA is rigid and has a crystalline structure, which can lead to the proper mechanical resistance. However, PE shows high gas permeability primarily for CO_2. Pebax®1657 (40wt% PA and 60wt% PEO) is a unique matrix for CO_2 gas separation process as a result of its high thermal stability and high CO_2 permeability [13,29,42].

In present study, the new TFC and TFN membranes were developed using PSF, Pebax and POP particles to improve the CO_2 selectivity over CH_4 and N_2. Pebax and Pebax/POP solutions were coated on the porous PSF support prepared via phase inversion method. TFC and TFN membranes were characterized through FTIR, FESEM-EDX, TGA/DTG, DSC methods. Moreover, the TFC and TFNs performance in gas separation was studied and compared. In addition, the ability of each membrane in CO_2/CH_4 and CO_2/N_2 separation was tested and discussed in various feed pressures. Finally, the outcomes attained in this study were compared with further similar studies.

2. Experimental

2.1. Materials

Methylbenzene (99.8) monomer, 1, 2-dichloroethane (DCE, ≥ 99.8%) nonpolar solvent, formaldehyde dimethyl-acetal (FDA, ≥ 99.0%) as cross-linker, and anhydrous ferric chloride ($FeCl_3$ ≥ 99.0%) catalyzer was supplied from Sigma-Aldrich. Pebax®1657 powder as a continuous phase of selective layer of membrane was purchased from Arkema (France). Polysulfone was provided from BASF (Germany) and used to fabricate the support of TFN. Solvents including ethanol (99.99%), dimethyl-form-amide (DMF) were obtained from Merck Company.

2.2. Synthesis of POP-CH_3

To synthesize POP-CH_3 via Friedel-Crafts method, methylbenzene (0.02 mol, 1.84 g) and FDA (0.06 mol, 4.6 g) were added into 25 mL of DCE, drop-wisely. After stirring for 20 min, anhydrous $FeCl_3$ (0.04 mol, 4.5 g) was added under a nitrogen environment which continued for 10 min. After 15 min of stirring, the resulting reaction mixture was poured into an autoclave (35 ml) and heated at 353 K for 1 day in an oven. After cooling to ambient temperature, the obtained brown jellylike sediment was filtered by centrifugation and then washed with methanol seven times. Consequently, the precipitate was dried overnight at ambient condition and then purified by Soxhlet extraction in methanol at 348 K for 1 day. Eventually, the product was dried at 333 K in vacuum oven to obtain a black POP-CH_3 particles [43].

2.3. Preparation of modified TFN membranes

The PSF sublayer was synthesized via phase inversion procedure. A definite amount of PSF was used to prepare a solution of 15 wt. % PSF in DMF solvent and then kept at stationary for 2 h to eliminate air bubbles. The final homogenous solution was casted on the clean glass plate with the thickness of 400 µm and then submerged in the deionized water bath for 24 h for solvent/nonsolvent exchange. The porous PSF support membrane has detached and dried 24 h in an oven at 313 K. The TFN synthesis was conducted through coating a Pebax/POPCH_3 thin layer over the porous support. First, a specific amount of synthesized POP-CH_3 was added into deionized water/ethanol mixture (30/70 w/w) and stirred for 5 hr to establish a homogenous suspension. Afterward, the suspension was sonicated in order to prevent particles aggregation. Subsequently, Pebax polymer (5 wt. %) was added into POP/solvent suspension. The uniform solution of 5 wt.% of Pebax found after 24 h stirring. To prepare TFN membrane, the porous PSF support was immerged in the Pebax/POP-CH_3 solution for 5 min and this was repeated for three times to acquire the Pebax/POP-CH_3 suitable thickness. Finally, the Pebax/POP-CH_3 coated PSF membrane was heated in an oven at 313 K for 12 hr. TFN membranes composition are tabulated in Table 1.

2.4. POP-CH_3 and membranes characterization

FTIR spectrometer (FTIR, Thermo scientific, USA) was employed to explore the functional groups of POP-CH_3, TFC and modified TFN membranes. The spectra were regularized in the wavenumber range of 400 – 4400 cm^{-1}. The BET analysis (Belsorp mini, Japan) was applied to investigate the textural properties of synthesized POP particles. Thermal gravimetric analysis/derivative thermo gravimetry (TGA/DTG, Mettler Toledo, USA) was

used to study the membranes thermal stability. The TFC and TFN membrane were heated under nitrogen atmosphere in the temperature range of 20 °C to 700 °C with the rate of 10 °C/min^{-1}. In addition, double scans of differential scanning calorimetry analysis (DSC, Mettler Toledo, USA) were utilized by applying a Perkin Elmer 8000 differential scanning calorimeter. The TFN membranes samples were kept stable in an alumina pan and heated up to 250 K with the rate of 10 °C/min. Subsequently, the membranes were cooled down to ambient temperature and then reheated to 250 °C again. The morphology of synthesized POP-CH_3 and also the prepared TFC and TFN membranes was studied by means of field emission scanning electron microscope (FESEM, MIRA3TESCAN-XMU, Czech Republic).

2.5. Gas permeation experiment

To investigate the separation characteristics of TFC and modified TFN membranes, the pure gas (i.e., N_2, CH_4 and CO_2) permeation test was conducted at various feed pressure and temperature at 30 °C. The gases permeability was determined utilizing Eq. 1 as follow:

$$P = \frac{273.15t10^{10}V}{760*76ATP}\left(\frac{dp}{dt}\right) \quad (1)$$

where P parameter is the pure gases permeability in terms of Barrer unit, t is the thickness of membrane (cm), V is the vessel volume (cm^3), A demonstrates the efficient membrane area (cm^2). p parameter is the applied pressure of feed and dp/dt represents the gradient of pressure change (mmHg/s). The ideal selectivity (α) could be expressed as below:

$$\alpha = \left(\frac{P_A}{P_B}\right) \quad (2)$$

where P_A and P_B are defined as pure gases permeability.

3. Results and discussion

3.1. Characterization of POP-CH_3 and modified TFN membranes

FTIR spectrum of each POP-CH_3, TFC and modified TFN membranes sample was illustrated in Figure 1. The weak bond in the range of 2950 cm^{-1} assign to the (C – H) bond stretching of methyl group in POP-CH_3 [43]. For PSF, the adsorption bands between 1168 cm^{-1} and 1325 cm^{-1} refer to the SO_2 symmetric and asymmetric stretch; respectively. Peak at 1320 cm^{-1} attributes to the (C–O) stretching. In addition, peaks at 1380 cm^{-1} and 1583 cm^{-1} relate to asymmetric (–CH_3) and (C=C); respectively [44].

To characterize PPPC-X, as was expressed Pebax involves two PA and PE fragments. Peaks at 870 cm^{-1} and 1122 cm^{-1} are related to (C – O – C) group bonds in PE and peaks at 1732 cm^{-1} refer to carbonyl group (C=O) in PA layer. As regards, the bands at 1490 cm^{-1}, 1645 and 3300 cm^{-1} are ascribed to C–N, H– N– C=O and N– H groups; respectively. Peaks at 2450 cm^{-1} and 2750 cm^{-1} are associated to symmetric and asymmetric C–H groups in Pebax polymer; respectively. Furthermore, the peak at 3510 cm^{-1} is the stretching refer to (O – H) group in Pebax polymer [45,46].

The physical properties of POP-CH_3 in terms of total pore volume, surface area and pore size found from BET analysis are tabulated in Table 2. As can be seen in Table 2, total pore volume, specific surface area and pore size of synthesized POP-CH_3 are 0.163 cm^3 g^{-1}, 151.06 m^2 g^{-1} and 4.32 nm; respectively.

Table 1
The TFC and modified TFN membranes composition

Membrane	Polymer (5 wt.%)		Solvent (wt.%) ethanol/deionized water (70/30 wt.%)	Code
	Pebax	POP		
PSF/Pebax	100	0	96	PP
PSF/Pebax_POP-CH_3	99	1	96	PPPC-1
PSF/Pebax_POP-CH_3	98	2	96	PPPC-2
PSF/Pebax_POP-CH_3	97	3	96	PPPC-3
PSF/Pebax_POP-CH_3	96	4	96	PPPC-4
PSF/Pebax_POP-CH_3	95	5	96	PPPC-5

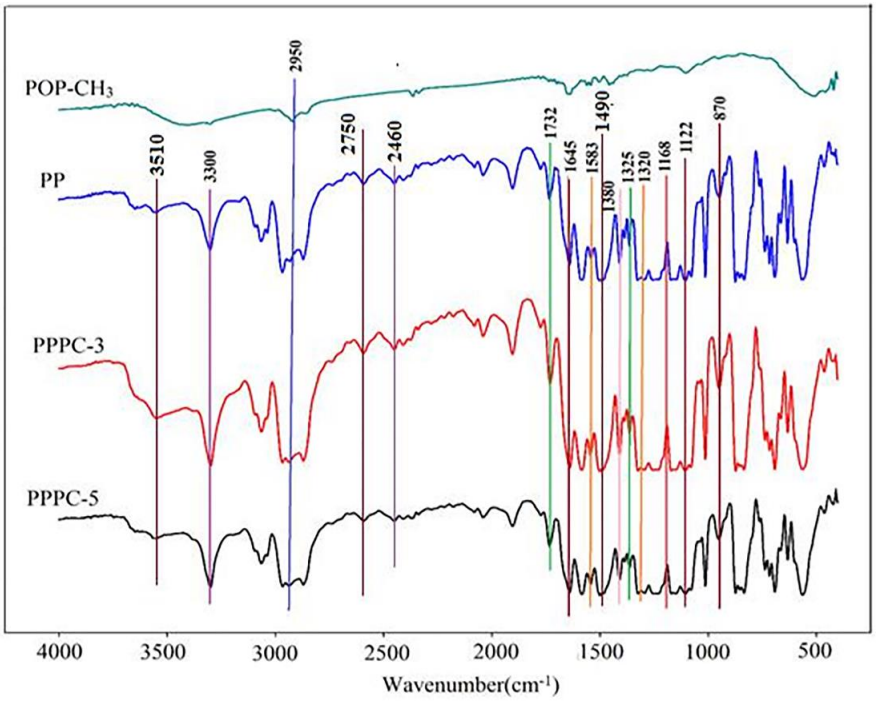

Fig. 1. FTIR spectra of POP-CH3, PP, PPPC-3 and PPPC-5.

Table 2
The results of BET analysis of POP-CH_3 particles.

Sample	S_{BET} (m^2 g^{-1})	V_{total} (cm^3 g^{-1})	D_p (nm)
POP-CH_3	151.06	0.163	4.32

FESEM used to survey the morphology of synthesized POP-CH_3 and also TFC and TFN membranes to investigate the quality of POP-CH_3 dispersion within the polymer matrix and the polymer/filler interface. Figure 2 shows the surface images of POP-CH_3 and depicts the cross-sectional images of PP and PPPC-X composite membranes with various POP-CH_3 incorporation.

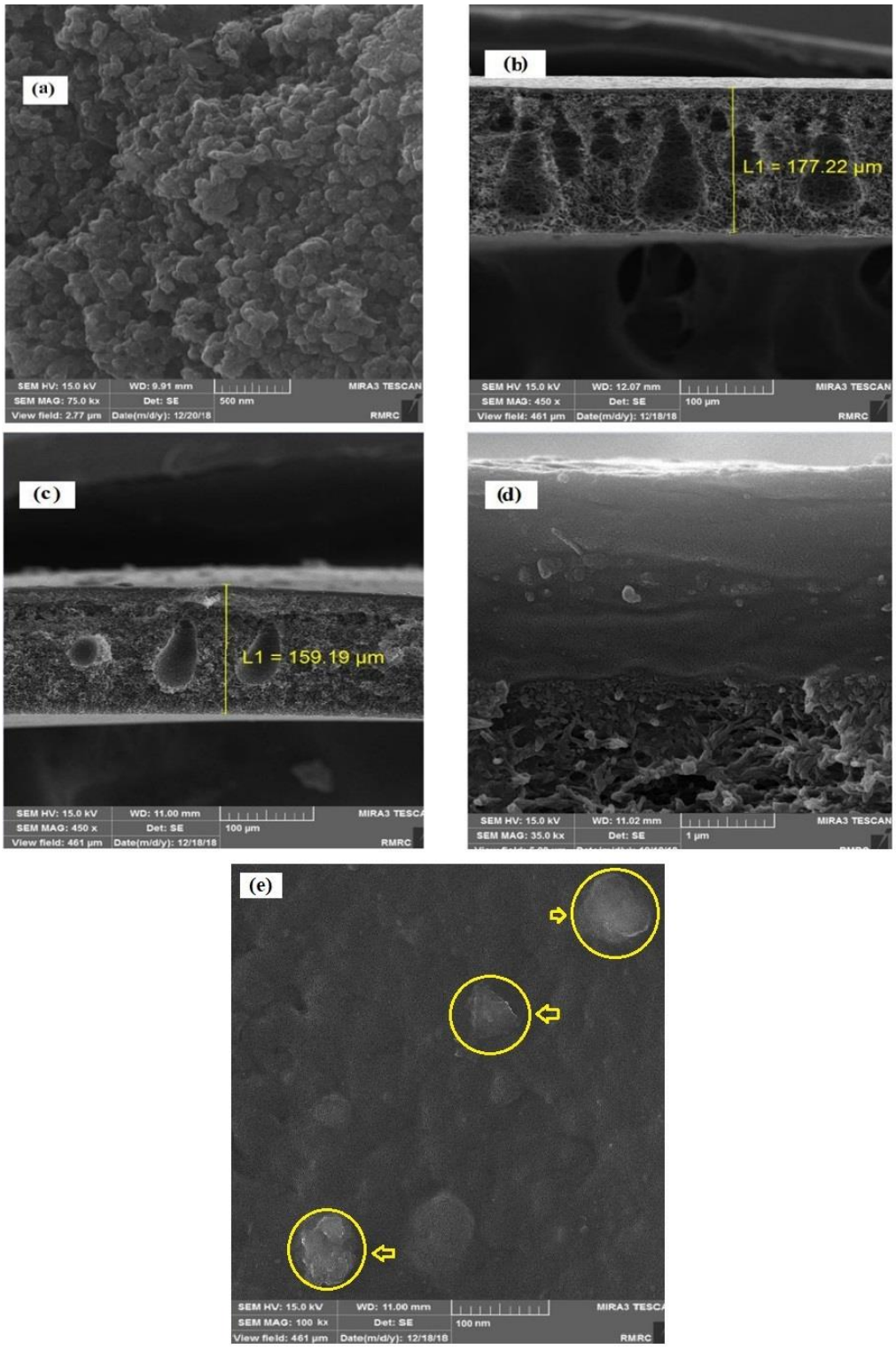

Fig. 2. FE-SEM images (a) surface of POP-CH_3; (b) low magnification cross sectional of PP; (c) low magnification cross sectional of PPPC-3; (d) the cross-sectional quality of Pebax layer and PSF support for PPPC-5; (e) a sample interface of POP and Pebax.

The aspect and size of the fillers was similar to some extent, as it was observed by SEM (Figure 2a). POP-CH_3 particles showed a morphology consisting on aggregates of sphere-shaped structures of different size and roughness. According to Figure 2b,c, Pebax top layer was well coated on the PSF sublayer and created a defect–free boundary. The Pebax layer thickness is much thinner than PSF one that can be utilized as a highly selective and permeable layer for CO_2 penetrant. The total thickness of membranes consisting PSF sublayer and selective Pebax layer for PP and PPPC-5 membranes were 177.22 and 159.16 μm, respectively. The cross-sectional images of selective layer of PPPC-5 membrane are demonstrated in Figure 2d. As can be observed, the interface of top layer and porous sublayer has an appropriate pattern with no defect. Nevertheless, as $POPCH_3$ particles loading is enhanced within the polymer matrix up to 5 wt.%, undesirable aggregation of POP-CH_3 were seen. In fact, particles loading of 5 wt.% is the percolation point due to aggregation of particles which can lead to selectivity decline for TFN membranes [47]. The quality of polymer/filler interface in composite membrane has been known as a key parameter that influences on the gas separation performance of membrane. An interface with no macro-void is a proper morphology which improves the gas separation properties of membrane. Figure 2e depicted a sample of polymer/filler interface of Pebax and POP-CH_3 which confirmed that there is an appropriate interface exists between them with no non-selective voids as can be possible.

The SEM-EDX was carried out to verify the presence of POP-CH_3 in the modified TFN membrane. Figure 3 shows the SEM-EDX results of synthesized POP-CH_3, PP, PPPC-3 and PPPC-5 which represented the existence of C, Fe, Cl, N and O elements in the membranes.

TGA was employed to illustrate the thermal stability of the synthesized membranes. Thermographs acquired for PPPC-X membranes with 3 and 5 wt.% of POP-CH_3 are displayed in Figure 4a. The TGA curves of TFC and TFN membranes consist of three stages. The initial decomposition stage of TFC and TFN membrane samples which is related to solvent evaporation which continued to around 100°C. The second step which assigned to the polymer chains degradation is different for synthesized membranes and as Figure 4a shows the decomposition temperature of membranes filled with 3 and 5 wt.% of POP-CH_3 decreases compare to TFC membrane. In addition, final decomposition of TFC and TFN membrane illustrated carbonization stage. In fact, these results demonstrated the proper thermal stability of TFC membrane compared to TFN membrane with 3 and 5 wt.% of $POPCH_3$ filler [48].

According to the Figure 4a, modified TFN membranes have been completely degraded in comparison to the neat membranes, so that for the membrane containing 5 wt.% of adsorbent occurred later than the membrane containing 3 wt.% adsorbent degradation, so it can be concluded that increasing the concentration of adsorbent causes later membranes to degrade and collapse [49,50].

The DTG curve which is the derivative of the thermometer curve is shown in Figure 4b. It also allows the maximum free fall temperature (T_{max}) to be set at a fast rate, which is then given T_e (start) and T_f (hidden temperature). All three temperatures change with changing test conditions. The surface below the DTG curve is proportional to the change in mass. DTG courier height at any temperature will change the speed of mass at that temperature. It is noteworthy that the amount of mass that is affected by the membrane in the time and temperature unit has been increased by increasing the amount of POP-CH_3 adsorbent and the effect of heat changes on synthesized PPPC-X membranes has been greater for adsorbent mixed matrix membranes [51]. DSC was carried out to examine the thermal properties of membranes in terms of crystallization temperature (T_c), melting temperature (T_m) and glass transition temperature (T_g). The analysis was performed with three replications and the average data were reported.

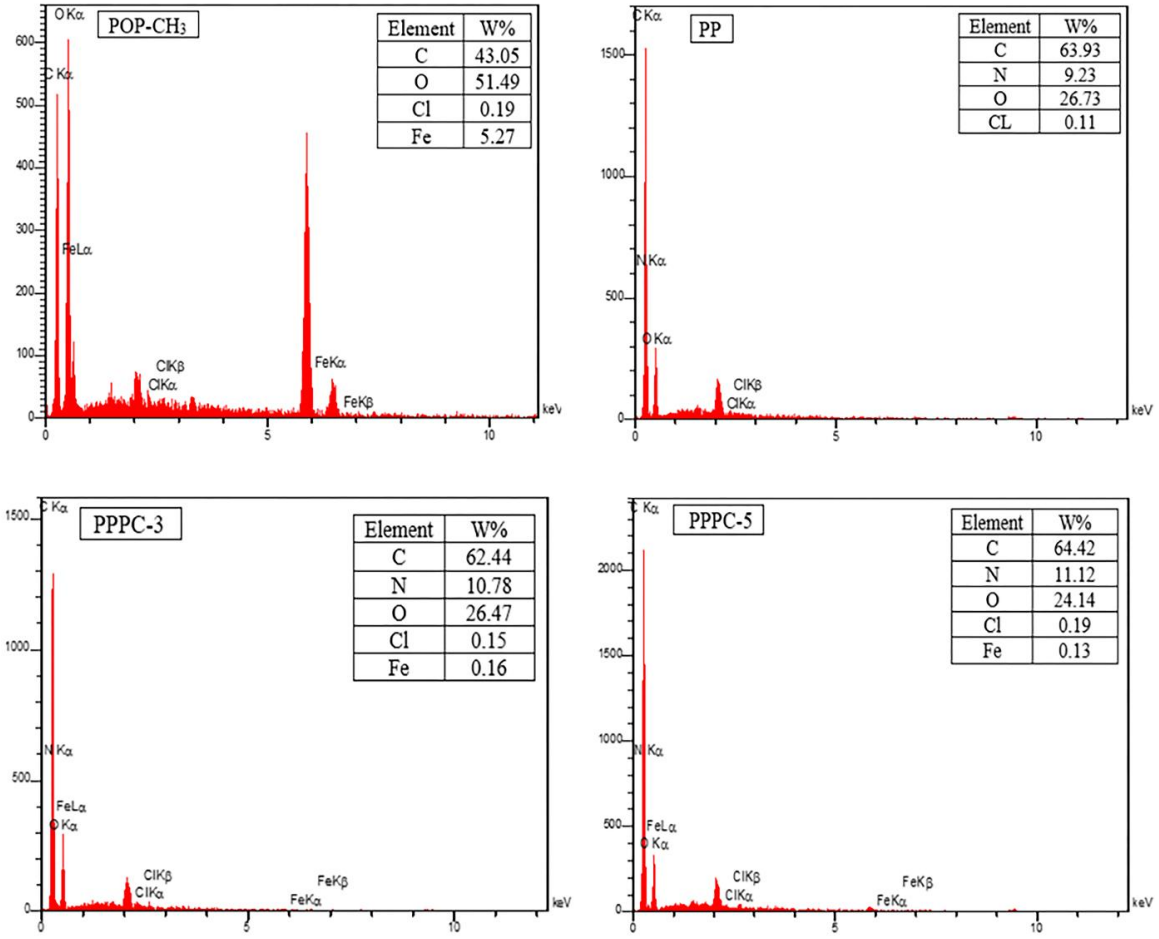

Fig. 3. SEM-EDX of POP-CH3, PP, PPPC-3 and PPPC-5.

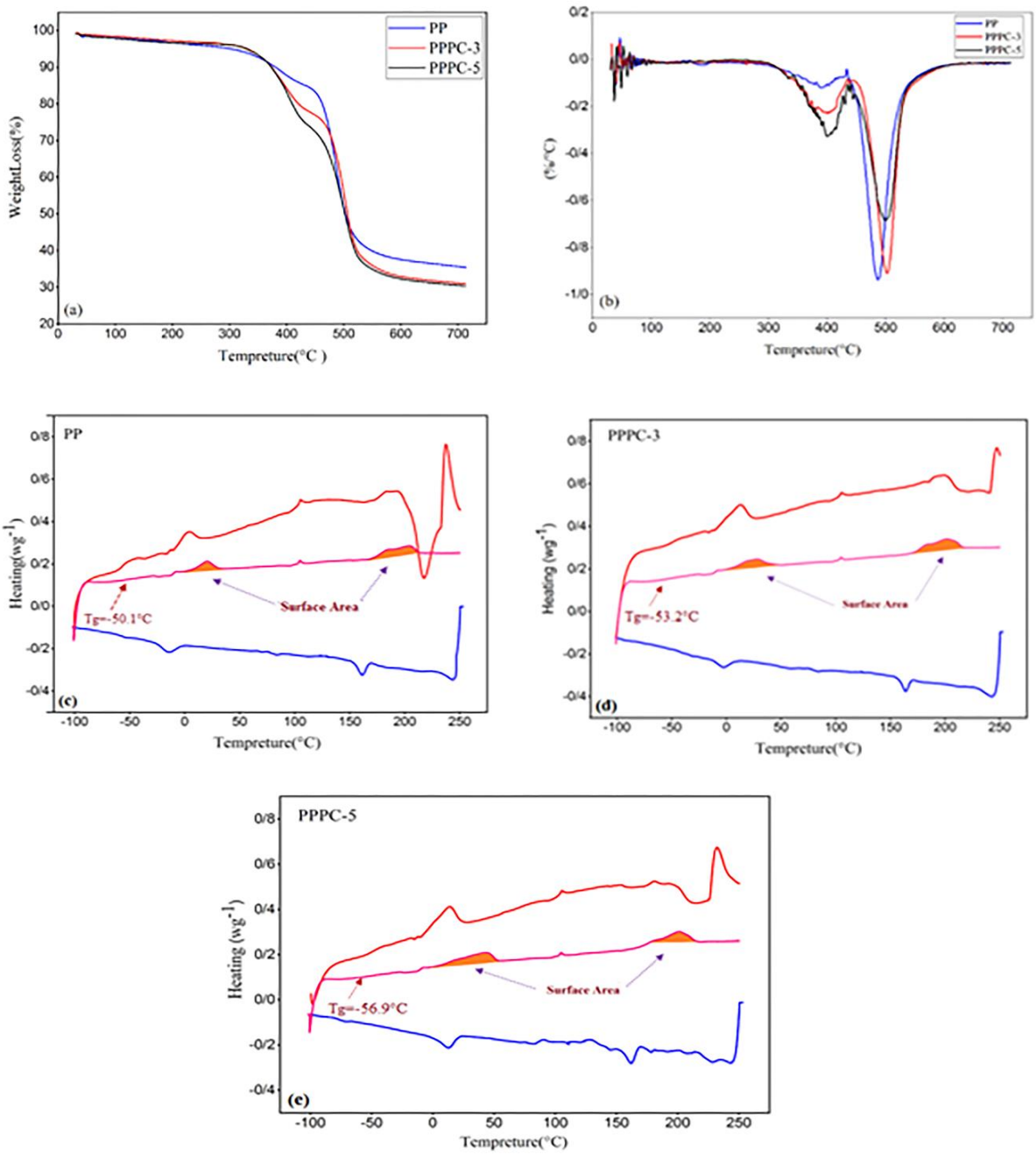

Fig. 4. (a) TGA curve of PP, PPPC-3, PPPC-5. PPPC-5; (b) DTG thermographs of PP, PPPC- 3, PPPC-5; (c, d, e) DSC thermographs of PP, PPPC-3, PPPC-5.

T_g and T_m are a function of polymeric chains and intermolecular interactions; respectively. The DSC thermograph for the PP, PPPC-3 and PPPC-5 membranes are demonstrated in Figure 4c-e. The thermal properties including T_g and T_m of some membranes are reported in Table 3. The T_g of membranes decreased from -50.1°C for PP to -53.2°C and -56.9°C for PPPC-3 and PPPC-5, respectively. Decreasing in T_g reflects the variation in polymer chains long-range mobility. It can be concluding that, owing to the low mobility of synthesized POP-CH_3 and higher stiffness of these particles, the polymer chains mobility would restrict and the T_g parameter of Pebax containing POP membranes would decrease [46]. Moreover, the DSC curves show the melting temperature of membranes. It is evident that for all membranes, the T_m of PA segment is higher than PEO one. The inter-block hydrogen bond in PA is responsible for higher T_m which ultimately increases the energy required for phase change. The T_m of both PEO and PA increases for Pebax containing POP particles.

Table 3
Glass transition and melting temperatures of TFC and selected TFN membranes.

Membrane	T_g (°C)	$T_{m,PEO}$ (°C)	$T_{m,PA}$ (°C)
PP	-50.1	20.7	203.5
PPPC-3	-53.2	28.5	202.3
PPPC-5	-56.9	43	201.1

3.2. Gas permeation study

The permeability measurement of CO_2, CH_4 and N_2 gases was conducted at 30 °C and various applied feed pressure with three replications to examine the permeation properties of TFC and TFN membranes. A series of gas permeation tests were design to investigate the impact of both applied feed pressure and POP-CH_3 loading on the gas separation efficiency of TFC and modified TFN membranes. The properties of each studied gases are tabulated in Table 4.

3.2.1. Effect of POP-CH_3

Figure 5a depicts the effect of POP-CH_3 on gases permeability for all TFC and TFN membranes. As can be seen, embedding the porous organic fillers into the membrane matrix can alter the permeation properties of modified TFN membranes. The outcomes illustrated that the CO_2 gas permeability was higher than N_2 and CH_4. The Kinetic diameter of the penetrants as well as the condensation property affect the rate of gas permeability. Condensation is defined by the critical temperature and the condensability means the gas interest to adsorb by polymer chains. As can be observed in Table 4, CO_2 molecules are more condensable as an outcome of the higher critical temperature than N_2 and CH_4. Therefore, CO_2 gas molecules showed greater permeability than N_2 and CH_4 due to higher condensability and lower Kinetic diameter [29]. Moreover, the interaction among quadrupole carbon dioxide and PA segment of Pebax can lead to the high CO_2 permeation [10].

The affinity of other types of POP to adsorb CO_2 molecules are reported previously. Sun et al. synthesized two benzoxazine-containing porous organic polymer (BPOP-1, BPOP-2) by using Sonogashira-Hagihara coupling reactions based on tetrahedral silicon-centered monomer and brominated benzoxazine. The existence of benzoxazine with oxygen and nitrogen atoms in the network provided high CO_2 sorption [37]. Sun et al. also synthesized two ferrocene-containing microporous polymers (FPOP-1 and FPOP-2) by using Sonogashira-Hagihara coupling reactions of 1,1-diethynylferrocene with tetrakis (4-bromophenyl) silane or tri(4-bromophenyl) phenylsilane. The existence of ferrocene in the network can lead to high CO_2 uptake as a result of the good interaction between electron-rich CO_2 gas and withdrawing electron ferrocene [38].

Regarding Figure 5a, pure CO_2, CH_4 and N_2 gases permeability for neat TFC membrane at feed pressure of 2 bar were 218.1, 21.3 and 3.3 Barrer; respectively and increased up to 310.6, 27.6 and 4.5 Barrer for PPPC-5 membrane. All pure gases permeability demonstrated an increasing trend. Increasing fractional free volume (FFV) of PPPC-X membranes due to the filler addition, enhances the permeability, especially for the smaller gas [10]. This increasing trend indicates interaction between nucleophilic property of methylbenzene's benzene ring of POP-CH_3 and electrophilic property of CO_2. Figure 6 represents the interaction among CO_2 and POP-CH_3 particles which accelerate the permeation of CO_2 thorough the TFN. As can be seen, POP-CH_3 can improve the CO_2 permeability via two scenarios. CO_2 with a lower kinetic size has more chance than CH_4 to path through POP pores and also the nucleophilic-electrophilic interaction among benzene ring and CO_2 enhances the CO_2 permeability. According to Figure 5b, CO_2/CH_4 selectivity is lower than CO_2/N_2 selectivity due to lower N_2 permeability in all neat TFC and TFN membrane. The embedded POP-CH_3 particles improve the sorption properties of all TFN membrane, especially for CO_2. Thus, the interaction between CO_2 molecules and Pebax polar groups joined with CO_2 sorption by POP-CH_3 with CO_2 would increase the CO_2/N_2 and CO_2/CH_4 selectivity.

As can be seen in Figure 5b, CO_2/CH_4 gas selectivity for neat TFC membrane at applied feed pressure of 2 bar was 10.01 and increased up to 11.25 for PPPC-5 membrane. In addition, CO_2/N_2 selectivity for PP at feed pressure of 200 kPa was 65.54 and increased up to 70.04 for membrane with 5 wt.% POP-CH_3 loading. These results also confirm the proper compatibility and adhesion between Pebax and the POP-CH_3.

3.2.2. Effect of feed pressure

Figures 7 and 8 demonstrate the effect of feed pressure on CO_2/CH_4 and CO_2/N_2 selectivity and gases permeability for TFC and modified TFN membranes. As can be observed in Figure 7, the TFC membrane permeability for N_2, CH_4 and CO_2 was increased from 218.1, 21.3 and 3.3 Barrer to 241.6, 22.9 and 3.5 Barrer, respectively; as the feed pressure increases from 2 to 10 bar. The permeability of all gases also show improvement at intermediate pressure of 6 bar. The N_2, CH_4 and CO_2 gases permeability for TFC membrane were improved to 230.2, 22.4 and 3.4 Barrer, respectively; at 6 bar. As regards, permeability of carbon dioxide raised for all TFN membranes also showed ascending trend as the applied pressure enhances from 2 to 10 bar. The PPPC-5 permeability for CO_2 raised from 310.6 Barrer at 2 bar to 322.8 Barrer at 6 bar and this improvement continued to 348.4 Barrer by increasing feed up to 10 bar. The carbon dioxide concentration within the polymer matrix increases by applying higher feed pressure which can results in plasticization effect. However, the N_2 and CH_4 permeability for TFNs reduced as feed pressure increased. The permeability of PPPC-5 for N_2 and CH_4 decreased from 27.6 and 4.5 Barrer to 24.8 and 3.7 Barrer; respectively. N_2 and CH_4 gases permeate through the modified TFNs with dominant diffusion and their permeability decrease as the applied feed pressure increased. Higher feed pressure can lead to polymer chains compactness and thus confining the penetrant diffusion.

Table 4
Physical characteristics of studied gases [51].

Gas	Molecular weight (g/mol)	Kinetic diameter (Å)	Critical temperature (°C)
CO_2	44.01	3.3	31.2
CH_4	16.04	3.8	-82.1
N_2	28.01	3.64	-147.1

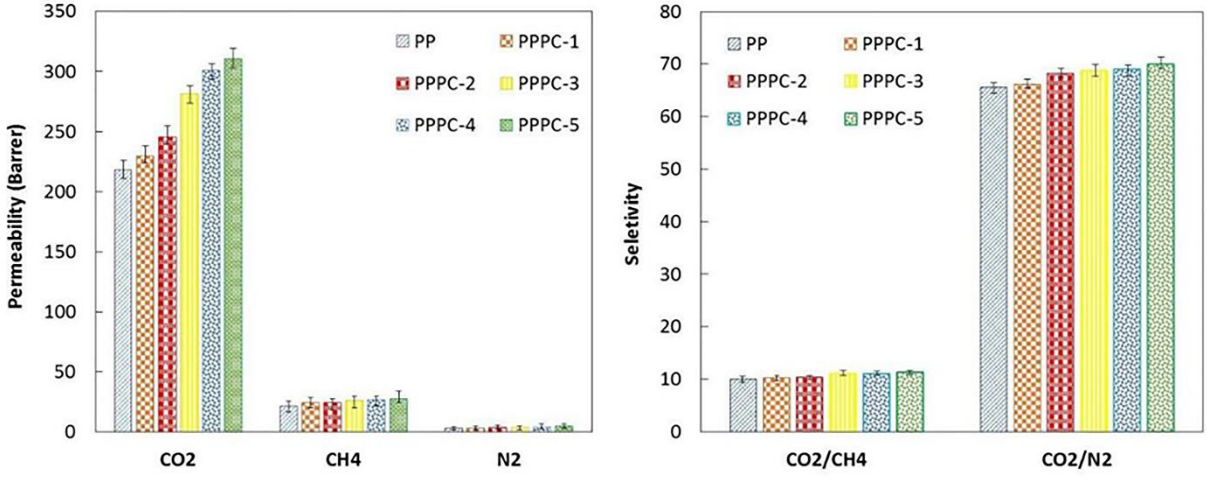

Fig. 5. Effect of embedded POP-CH_3 on N_2, CH_4 and CO_2 permeability and also on CO_2/N_2 and CO_2/CH_4 selectivity at 30°C and pressure 2 bar for all synthesized membranes.

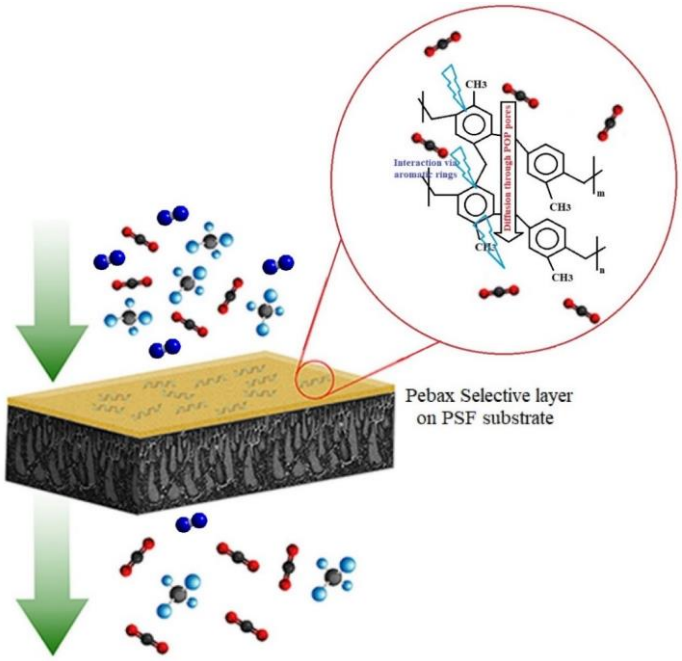

Fig. 6. Schematic representation of interaction among CO_2 and POP-CH_3 in TFN membranes.

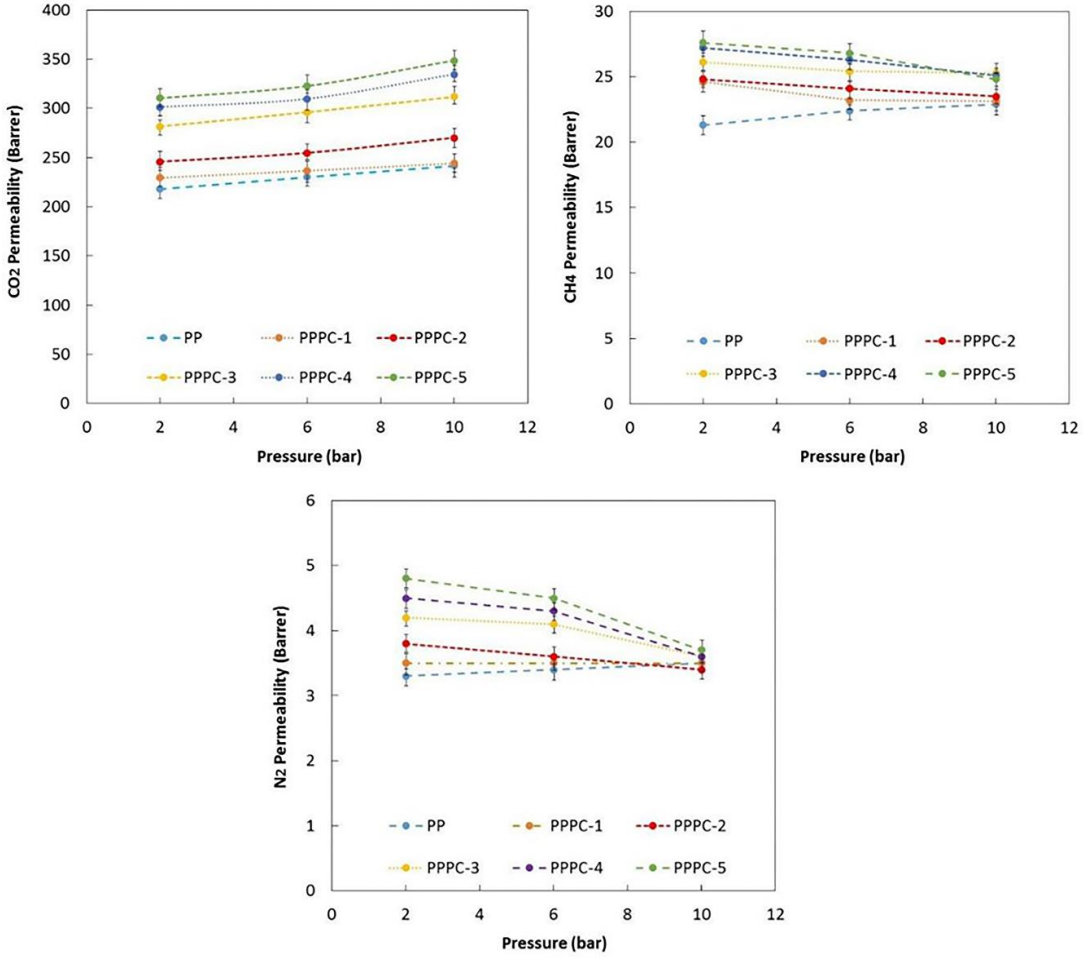

Fig. 7. The effect of applied pressure on CO_2, CH_4 and N_2 permeability of TFC and modified TFN membranes.

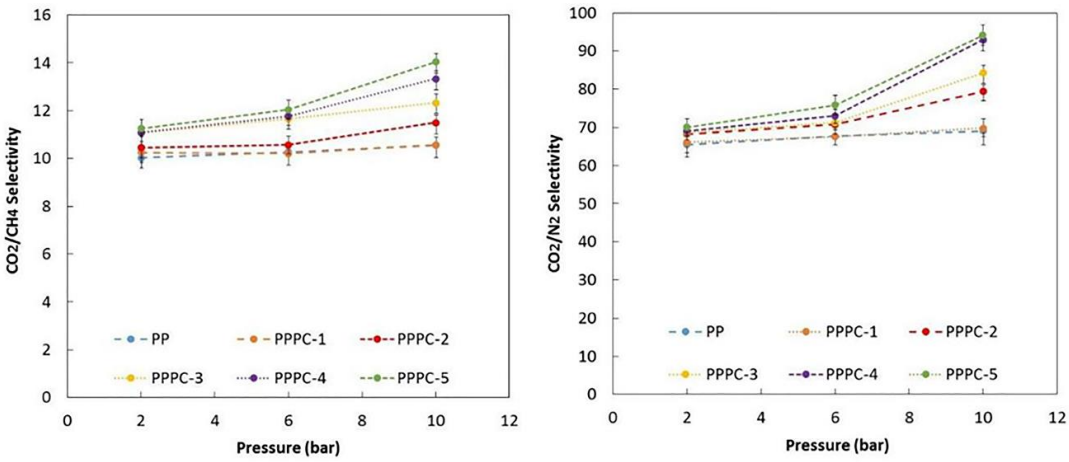

Fig. 8. The effect of applied pressure on CO_2/CH_4 and CO_2/N_2 selectivity of TFC and modified TFN membranes.

The permeability is the multiplication of solubility coefficient and diffusion coefficient. According to the dual sorption model, the diffusion coefficient reduces due to compactness of polymer chains before the plasticization effect [2,29]. The amount of CO_2 sorption is increased by applying higher feed pressure. In fact, the competition between POP-CH_3 intensity to sorb CO_2 and polymer chain compactness which hinders the penetrant diffusion consequences to the higher CO_2 permeability and on the other hands, prevents the N_2 and CH_4 permeation. Therefore, the trend of pure gas permeability illustrated that the CO_2 sorption by POP-CH_3 has greater influence on CO_2 permeability at higher feed pressure.

Figure 8 illustrates that the CO_2/N_2 and CO_2/CH_4 selectivities also enhanced by enhancing the applied pressure for all TFC and TFN membranes. The CO_2/CH_4 and CO_2/N_2 gases selectivities for PP membrane were 10.01 and 65.54 at 2 bar respectively. The CO_2/N_2 and CO_2/CH_4 gases selectivities for PPPC-5 enhanced from 11.25 and 70.04 to 12.04 and 75.73, respectively as the applied pressure enhanced from 200 to 600 kPa. The best selectivity achieved at applied feed pressure of 10 bar, in which the CO_2/CH_4 and CO_2/N_2 gases selectivities enhanced to 14.04 and 94.16, respectively.

3.2.3. Gas separation performance

The ability of different fillers for CO_2/CH_4 and CO_2/N_2 gases separation is tabulated in Table 5. According to the exhibited data, as various fillers were added to polymer matrix, pure gases permeability and selectivity improved and all studies demonstrated a trade-off relationship between the pure gas's selectivity and permeability. As can be observed from Table 5, the separation efficiency of all membrane is a great function of polymer type, fillers and process condition. Usually, the membranes with appropriate selectivity and high permeability are more attractive for industrial application. Based on the data presented in Table 5, the best efficiency obtained in this work was the CO_2 permeability of 348.4 Barrer and the CO_2/N_2 and CO_2/CH_4 gases selectivity of 94.16 and 14.04, respectively; all at applied pressure of 10 bar and temperature of 30 °C.

Figure 9 represents the Robeson bound in CO_2/N_2 separation and the efficiency of TFC and modified TFN membranes for CO_2 gas separation from N_2 gas. As Figure 9 depicted, the improvement of membrane's performance depends on feed pressure and the loading of embedded POP particles. Both factors have synergetic effect on CO_2/N_2 selectivity and CO_2 gas permeability. It can be observed that, adding the POP incorporating within the Pebax along with rising applied feed pressure make condition to overcome the Robeson bound in CO_2/N_2 separation.

4. Conclusions

A TFN membrane comprising selective Pebax layer filled with POP-CH_3 supported by polysulfone was fabricated to specify the effect of POP-CH_3 incorporation on the characteristics and gases separation efficiency of the synthesized membranes. Outcomes indicated that the uniform particle dispersion was obtained with proper interface quality. This proper interface results from the strong interaction between POP particles and Pebax chain as described in FTIR analysis. Incorporating the POP-CH_3 within the Pebax top layer causes high CO_2/CH_4 and CO_2/N_2 selectivity and CO_2 gas permeability as a result of the strong affinity of POP-CH_3 toward polar CO_2 gas. The permeation attributes of all membranes were studied in the applied feed pressure range of 2 – 10 bar. The permeability of TFC membrane for N_2, CO_2 and CH_4 were enhanced as the applied feed pressure increased and reached to 241.6, 22.9 and 3.5 Barrer, respectively at applied feed pressure of 10 bar. A similar ascending trend was seen for TFN membranes and the gases permeability increased at higher applied feed pressure. The best selectivity and permeability were obtained at 5 wt.% loading of POP-CH_3 for all tested gases. The CO_2/N_2 and CO_2/CH_4 selectivity of TFN membranes enhanced from 10.55 and 69.02 to 14.04 and 94.16, respectively; at applied feed pressure of 10 bar by enhancing POP-CH_3 loading to 5 wt.%. The results of CO_2/N_2 separation performance were compared with Robeson upper bound. It was concluded that the increment in POP loading and applying higher applied pressure made a condition to overcome the Robeson bound.

Table 5
A comparison between the gas separation performances of modified TFN membranes with some selected works.

Polymer	Filler	Loading (wt.%)	Condition		P_{CO2} (Barrer)	P_{CH4} (Barrer)	P_{N2} (Barrer)	P_{CO2}/P_{CH4}	P_{CO2}/P_{N2}	Ref.
			P (bar)	T (°C)						
Pebax®1657	Fe-BTC	20	3	25	98.32	4.43	-	22.2	-	[27]
		40	3	25	425.	34.6		12.3		
Pebax®1657	Glycerol	15	10	25	50.42	-	0.82	-	61.5	[33]
PMP/Pebax	UiO-66	2	7	25	369.3	11.8	-	31.3	-	[52]
	UiO-66-NH_2	1.5			393.4	9.9		39.8		
PSF/Pebax	POP-CH_3	1	10	30	244.2	23.2	3.5	10.52	69.77	This work
	POP-CH_3	5			348.4	24.8	3.7	14.04	94.16	

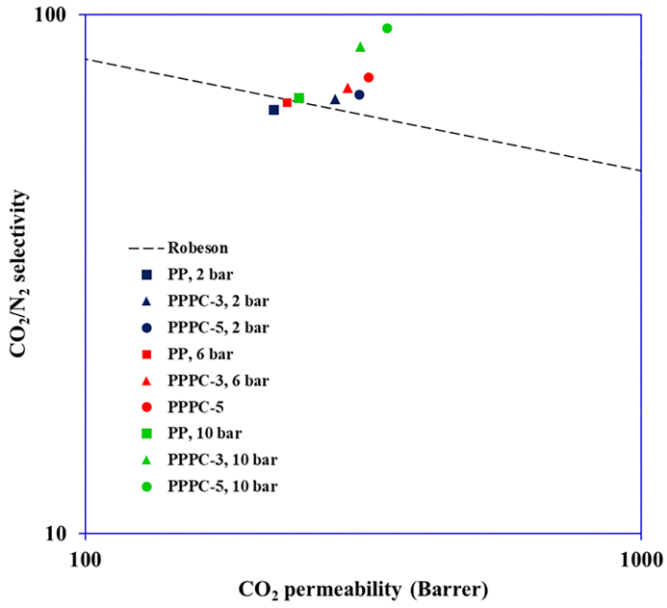

Fig. 9. The TFC and TFN membranes performance in CO_2/N_2 separation in comparison to Robeson bound.

Acknowledgment

The authors acknowledge Babol Noshirvani University of Technology for financial support of this project (Grant NO. BNUT/393054/2019).

Abbreviations

TFC	Thin film composite
TFN	Thin film nanocomposite
PSF	Polysulfone
PMP	Polymethyl pentyne
MMM	Mixed matrix membrane
POP	Porous organic polymers

References

[1] R. Abedini, M. Omidkhah, F. Dorosti, Highly permeable poly (4-methyl-1 pentyne)/NH_2-MIL 53 (Al) mixed matrix membrane for CO_2/CH_4 separation, RSC Adv. 4 (2014) 36522-36537, https://doi.org/10.1039/C4RA07030E.

[2] N.C. Su, D.T. Sun, C.M. Beavers, D.K. Britt, W.L. Queen, J.J. Urban, Enhanced permeation arising from dual transport pathways in hybrid polymer–MOF membranes, Energy. Env. Sci. 9 (2016) 922-931, https://doi.org/10.1039/C5EE02660A.

[3] M.H. Nematollahi, A.H. Saeedi Dehaghani, R. Abedini, CO_2/CH_4 separation with poly (4 methyl-1-pentyne) (TPX) based mixed matrix membrane filled with Al_2O_3 nanoparticles, Korean J. Chem. Eng. 33 (2016) 657-665, https://doi.org/10.1007/s11814-015-0168-x.

[4] M. Jamshidi, V. Pirouzfar, R. Abedini, M. Zamani Pedram, The influence of nanoparticles on gas transport properties of mixed matrix membranes: An experimental investigation and modeling, Korean J. Chem. Eng. 34 (2017) 829-843, https://doi.org/10.1007/s11814-016-0302-4.

[5] M. Salimi, V. Pirouzfar, E. Kianfar, Enhanced gas transport properties in silica nanoparticle filler-polystyrene nanocomposite membranes, Colloid Polym. Sci. 295 (2017) 215-226, https://doi.org/10.1007/s00396-016-3998-0.

[6] M. Kheirtalab, R. Abedini, M. Ghorbani. A novel ternary mixed matrix membrane comprising polyvinyl alcohol (PVA)-modified poly (ether-block-amide)(Pebax® 1657)/graphene oxide nanoparticles for CO_2 separation, Process Saf. Environ. Prot. 144 (2020) 208-224, https://doi.org/10.1016/j.psep.2020.07.027.

[7] M. R. S. Kebria, M. Jahanshahi, A. Rahimpour, SiO_2 modified polyethyleneimine based nanofiltration membranes for dye removal from aqueous and organic solutions, Desalination. 367 (2015) 255-264, https://doi.org/10.1016/j.desal.2015.04.017.

[8] M.H. Zhang, K. Wang, Y.J. Du, G. Dai, W. Sun, G. Li, High and temperature-insensitive piezoelectric strain in alkali niobate lead-free perovskite, J. Am. Chem. Soc. 139 (2017) 3889- 3895, https://doi.org/10.1021/jacs.7b00520.

[9] R. Abedini, A. Mosayebi, M. Mokhtari, Improved CO_2 separation of azide crosslinked PMP mixed matrix membrane embedded by nano-CuBTC metal organic framework, Process Saf. Environ. 114 (2018) 229-239, https://doi.org/10.1016/j.psep.2017.12.025.

[10] F. Dorosti, M. Omidkhah, R. Abedini, Enhanced CO_2/CH_4 separation properties of asymmetric mixed matrix membrane by incorporating nano-porous ZSM-5 and MIL-53 particles into Matrimid® 5218, J. Nat. Gas. Sci. Eng. 25 (2015) 88-102, https://doi.org/10.1016/j.jngse.2015.04.033.

[11] I.H. Arellano, P. Pendleton. Phenomenological analyses of carbon dioxide adsorption kinetics on supported zinc-functionalized ionic liquid hybrid sorbents, Chem. Eng. J. 288 (2016) 255-263, https://doi.org/10.1016/j.cej.2015.11.054.

[12] N. Ahmad, C. Leo, A.W. Mohammad, A. Ahmad, Interfacial sealing and functionalization of polysulfone/SAPO-34 mixed matrix membrane using acetate-based ionic liquid in post-impregnation for CO_2 capture, Sep. Purif. Tech. 197 (2018) 439-448, https://doi.org/10.1016/j.seppur.2017.12.054.

[13] R. Abedini, M. Omidkhah, F. Dorosti, CO_2/CH_4 Separation by a Mixed Matrix Membrane of Polymethylpentyne/MIL-53 Particles, Iranian J. Polym. Sci. Technol. 27 (2014) 337-351, https://doi.org/10.22063/JIPST.2014.1096.

[14] S. Heydari, V. Pirouzfar, The influence of synthesis parameters on the gas selectivity and permeability of carbon membranes: empirical modeling and process optimization using surface methodology, RSC Adv. 6 (2016) 14149-14163, https://doi.org/10.1039/C5RA27772H.

[15] M.H. Nematollahi, S. Babaei, R. Abedini, CO_2 separation over light gasses for nanocomposite membrane comprising modified polyurethane with SiO_2 nanoparticles, Korean J. Chem. Eng. 36 (2019) 763-779, 10.1007/s11814-019-0251-9.

[16] J. Albo, J. Wang, T. Tsuru, Application of interfacially polymerized polyamide composite membranes to isopropanol dehydration: Effect of membrane pre-treatment and temperature, J. Membr. Sci. 453 (2014) 384-393, https://doi.org/10.1016/j.memsci.2013.11.030.

[17] E. Nezhadmoghadam, M. Pourafshari Chenar, M. Omidkhah, A. Nezhadmoghadam, R. Abedini, Aminosilane grafted Matrimid 5218/nano-silica mixed matrix membrane for CO_2/light gasses separation, Korean J. Chem. Eng. 35 (2018) 526-534, https://doi.org/10.1016/j.memsci.2013.11.030.

[18] S. Khoshhal Salestan, A. Rahimpour, R. Abedini, Experimental and theoretical studies of biopolymers on the efficient CO_2/CH_4 separation of thin-film Pebax® 1657 membrane, Chem. Eng. Process. 163 (2021) 108366, https://doi.org/10.1016/j.cep.2021.108366.

[19] S. Anastasiou, N. Bhoria, J. Pokhrel, K.S.K. Reddy, C. Srinivasakannan, K. Wang, Metal-organic framework/graphene oxide composite fillers in mixed-matrix membranes for CO_2 separation, Mater. Chem. Phys. 212 (2018) 513-522, https://doi.org/10.1016/j.matchemphys.2018.03.064.

[20] S. Khoshhal Salestan, K. Pirzadeh, A. Rahimpour, R. Abedini, Poly (ether-block amide) Thin-Film Membranes Containing Functionalized MIL-101 MOFs for Efficient Separation of CO_2/CH_4, J. Env. Chem. Eng. 9 (2021) 105820, https://doi.org/10.1016/j.jece.2021.105820.

[21] D.W. Shin, S.H. Hyun, C.H. Cho, M.H. Han, Synthesis and CO_2/N_2 gas permeation characteristics of ZSM-5 zeolite membranes, Mic. Mes. Mat. 85 (2005) 313-323, https://doi.org/10.1016/j.micromeso.2005.06.035.

[22] M. Tsyurupa, L. Maslova, A. Andreeva, T. Mrachkovskaya, V. Davankov, Sorption of organic compounds from aqueous media by hypercrosslinked polystyrene sorbents 'Styrosorbrs. React. Polym. 25 (1995) 69-78, https://doi.org/10.1016/0923-1137(95)00021-A.

[23] W.Q. Wang, J. Wang, J.G. Chen, X.S. Fan, Z.T. Liu, Z.W. Liu, Synthesis of novel hyper-cross-linked polymers as adsorbent for removing organic pollutants from humid streams, Chem. Eng. J. 281 (2015) 34-41, https://doi.org/10.1016/j.cej.2015.06.095.

[24] X. Wang, H. Li, J. Huang, Adsorption of p-chlorophenol on three amino-modified hyper-cross-linked resins, J. Coll. Interf. Sci. 505 (2017) 585-592, https://doi.org/10.1016/j.jcis.2017.06.053.

[25] Z. Ke, Y. Cheng, S. Yang, F. Li, L. Ding, Modification of COF-108 via impregnation/functionalization and Li-doping for hydrogen storage at ambient temperature, Int. J. Hydrogen Energy. 42 (2017) 11461-11468, https://doi.org/10.1016/j.ijhydene.2017.01.143.

[26] F. Dorosti, A. Alizadehdakhel, Fabrication and investigation of PEBAX/Fe-BTC, a high permeable and CO_2 selective mixed matrix membrane, Chem. Eng. Res. Des. 136 (2018) 119- 28, https://doi.org/10.1016/j.cherd.2018.01.029.

[27] V. Nafisi, M-B. Hägg, Development of dual layer of ZIF-8/PEBAX-2533 mixed matrix membrane for CO_2 capture, J. Membr. Sci. 459 (2014) 244-255, https://doi.org/10.1016/j.memsci.2014.02.002.

[28] M. Mozafari, A. Rahimpour, R. Abedini, Exploiting the effects of zirconium-based metal organic framework decorated carbon nanofibers to improve CO_2/CH_4 separation performance of thin film nanocomposite membranes, J. Ind. Eng. Chem. 85 (2020) 102-110, https://doi.org/10.1016/j.jiec.2020.01.030.

[29] M. Laghaei, M. Sadeghi, B. Ghalei, M. Shahrooz, The role of compatibility between polymeric matrix and silane coupling agents on the performance of mixed matrix membranes: Polyethersulfone/MCM-41, J. Membr. Sci. 513 (2016) 20-32, https://doi.org/10.1016/j.memsci.2016.04.039.

[30] S. Majumdar, B. Tokay, V. Matrin-Gill, J. Campbell, Mg-MOF-74/Polyvinyl acetate (PVAc) mixed matrix membranes for CO_2 separation, Sep. Purif. Technol. 238 (2020) 116411, https://doi.org/10.1016/j.seppur.2019.116411.

[31] M. Raouf, R. Abedini, M. Omidkhah, E. Nezhadmoghadam, A favored CO_2 separation over light gases using mixed matrix membrane comprising polysulfone/polyethylene glycol and graphene hydroxyl nanoparticles, Process Saf. Environ. 133 (2020) 394-407, https://doi.org/10.1016/j.psep.2019.11.002.

[32] S. Bonakala, S. Balasubramanian, Structure–Property Relationships in Amorphous Microporous Polymers, J. Phys. Chem. B. 120 (2016) 557-565, https://doi.org/10.1021/acs.jpcb.5b08842.

[33] L. Rodríguez-Jard´on, M. Mar L´opez-Gonz´alez, M. Iglesias, E. Maya, Effect of porous organic polymers in gas separation properties of polycarbonate based mixed matrix membranes, J. Membr. Sci. 619 (2021) 118795, https://doi.org/10.1016/j.memsci.2020.118795.

[34] C. Soto, E. Torres-Cuevas, A. González-Ortega, L. Palacio, A. Lozano, B.D. Freeman, P. Prádanos, A. Hernández, Gas Separation by Mixed Matrix Membranes with Porous Organic Polymer Inclusions within o- Hydroxypolyamides Containing m-Terphenyl Moieties, Polymers. 13 (2021) 931 – 948, https://doi.org/10.3390/polym13060931.

[35] G. Li, Q. Liu, B. Xia, J. Huang, S. Li, Y. Guan, Synthesis of stable metal containing porous organic polymers for gas storage, Eur. Polym. J. 91 (2017) 242-247, https://doi.org/10.1016/j.eurpolymj.2017.03.014.

[36] X. Sun, J. Li, W. Wang, Q. Ma, Constructing benzoxazine-containing porous organic polymers for carbon dioxide and hydrogen sorption, Eur. Polym. J. 107 (2018) 89-95, https://doi.org/10.1016/j.eurpolymj.2018.07.043.

[37] X. Sun, Y. Qi, J. Li, W. Wang, Q. Ma, J. Liang, Ferrocene-linked porous organic polymers for carbon dioxide and hydrogen sorption, J. Organomet. Chem. 859 (2018) 117-123, https://doi.org/10.1016/j.jorganchem.2018.01.054.

[38] S. Xu, J. He, S. Jin, B. Tan, Heteroatom-rich porous organic polymers constructed by benzoxazine linkage with high carbon dioxide adsorption affinity, J. Coll. Interf. Sci. 509 (2018) 457-462, https://doi.org/10.1016/j.jcis.2017.09.009.

[39] Q. Wang, C. Yang, G. Zhang, L. Hu, P. Wang, Photocatalytic Fe-doped TiO_2/PSF composite UF membranes: Characterization and performance on BPA removal under visiblelight irradiation, Chem. Eng. J. 319 (2017) 39-47, https://doi.org/10.1016/j.cej.2017.02.145.

[40] F. Gao, J. Wang, H. Zhang, H. Jia, Z. Cui, G. Yang, Aged PVDF and PSF ultrafiltration membranes restored by functional polydopamine for adjustable pore sizes and fouling control, J. Membr. Sci. 570 (2019) 156-167, https://doi.org/10.1016/j.memsci.2018.10.037.

[41] G. Dong, J. Hou, J. Wang, Y. Zhang, V. Chen, J. Liu, Enhanced CO_2/N_2 separation by porous reduced graphene oxide/Pebax mixed matrix membranes, J. Membr. Sci. 520 (2016) 860-868, https://doi.org/10.1016/j.memsci.2016.08.059.

[42] Y. He, Q. Liu, J. Hu, C. Zhao, C. Peng, Q. Yang, Efficient removal of Pb (II) by amine functionalized porous organic polymer through post-synthetic modification, Sep. Purif. Tech. 180 (2017) 142-148, https://doi.org/10.1016/j.seppur.2017.01.026.

[43] M. Fakoori, A. Azdarpour, R. Abedini, B. Honarvar, Effect of Cu-MOFs incorporation on gas separation of Pebax thin film nanocomposite (TFN) membrane, Korean J. Chem. Eng. 22 (2021) 199-207, https://doi.org/10.1007/s11814-020-0636-9.

[44] H. Sanaeepur, R. Ahmadi, A. E. Amooghin, D. Ghanbari, A novel ternary mixed matrix membrane containing glycerol-modified poly (ether-block-amide)(Pebax1657)/copper nanoparticles for CO_2 separation, J. Membr. Sci. 38 (2019) 121-138, https://doi.org/10.1016/j.memsci.2018.12.012.

[45] H, Hosseinzadeh Beiragh, M. Omidkhah, R. Abedini, T. Khosravi, S. Pakseresht, Synthesis and characterization of poly (ether-block-amide) mixed matrix membranes incorporated by nanoporous ZSM-5 particles for CO_2/CH_4 separation, Asia-Pacific J. Chem. Eng. 11 (2016) 522-532, https://doi.org/10.1002/apj.1973.

[46] M.J.C. Ordoñez, Jr.K.J. Balkus, J.P. Ferraris, I.H. Musselman, Molecular sieving realized with ZIF-8/Matrimid® mixed-matrix membranes, J. Membr. Sci. 361 (2010) 28-37, https://doi.org/10.1016/j.memsci.2010.06.017.

[47] H. Zhao, L. Feng, X. Ding, Y. Zhao, X. Tan, Y. Zhang, The nitrogen-doped porous carbons/PIM mixed-matrix membranes for CO_2 separation, J. Membr. Sci. 564 (2018) 800-805, https://doi.org/10.1016/j.memsci.2018.07.075.

[48] M.Z. Rong, M.Q. Zhang, Y.X. Zheng, H.M. Zeng, K. Friedrich, Improvement of tensile properties of nano-SiO_2/PP composites in relation to percolation mechanism, Polymer. 42 (2001) 3301-3304, https://doi.org/10.1016/S0032-3861(00)00741-2.

[49] M.Z. Rong, M.Q. Zhang, Y.X. Zheng, H.M. Zeng, R. Walter, K. Friedrich, Structure–property relationships of irradiation grafted nano-inorganic particle filled polypropylene composites, Polymer. 42 (2001) 167-183, https://doi.org/10.1016/S0032-3861(00)00325-6.

[50] T. Khosravi, M. Omidkhah, Preparation of CO_2 selective composite membranes using Pebax/CuBTC/PEG-ran-PPG ternary system, J. Energy Chem. 26 (2017) 530-539, https://doi.org/10.1016/j.jechem.2016.10.013.

[51] A. Brunetti, F. Scura, G. Barbieri, E. Drioli, Membrane technologies for CO_2 separation, J. Membr. Sci. 359 (2010) 115–125, https://doi.org/10.1016/j.memsci.2009.11.040.

[52] M. Mozafari, R. Abedini, A. Rahimpour, Zr-MOFs incorporated thin film nanocomposite-Pebax 1657 membranes dip coated on polymethylpentyne layer for efficient separation of CO_2/CH_4, J. Mater. Chem. A. 6 (2018) 12380-12392, https://doi.org/10.1039/C8TA04806A.